

Click Assembly of Dye-Functionalized Octasilsesquioxanes for Highly Efficient and Photostable Photonic Systems

M. Eugenia Pérez-Ojeda,^[a] Beatriz Trastoy,^[b] Íñigo López-Arbeloa,^{*[c]} Jorge Bañuelos,^[c] Ángel Costela,^[a] Inmaculada García-Moreno,^{*[a]} and Jose Luis Chiara^{*[b]}

Dedicated to the memory of Professor Roberto Sastre

Abstract: New hybrid organic–inorganic dyes based on an azide-functionalized cubic octasilsesquioxane (POSS) as the inorganic part and a 4,4-difluoro-4-bora-3a,4a-diaza-*s*-indacene (BDP) chromophore as the organic component have been synthesized by copper(I)-catalyzed 1,3-dipolar cycloaddition of azides to alkynes. We have studied the effects of the linkage group of BDP to the POSS unit and the degree of functionalization of this inorganic core on the ensuing optical properties by comparison with model dyes. The high fluorescence of the BDP dye is preserved in spite of the linked chain

at its *meso* position, even after attaching one BDP moiety to the POSS core. The laser action of the new dyes has been analyzed under transversal pumping at 532 nm in both the liquid phase and when incorporated into solid polymeric matrices. The monosubstituted new hybrid dye exhibits high lasing efficiency of up to 56% with high photostability, with its laser output remaining at the initial value after 4×10^5 pump

pulses in the same position of the sample at a repetition rate of 30 Hz. However, functionalization of the POSS core with eight fluorophores leads to dye aggregation, as quantum mechanical simulation has revealed, worsening the optical properties and extinguishing the laser action. The new hybrid systems based on dye-linked POSS nanoparticles open up the possibility of using these new photonic materials as alternative sources for optoelectronic devices, competing with dendronized or grafted polymers.

Keywords: azides • click chemistry • dyes/pigments • hybrids • silsesquioxanes

Introduction

Fully condensed polyhedral oligosilsesquioxanes (POSS) are unique nanometer-sized hybrid inorganic–organic materials of chemical composition $(\text{RSiO}_{1.5})_n$, which can be readily synthesized by hydrolytic condensation of trifunctional organosilicon monomers RSiX_3 (R = organic group; X = halogen

or alkoxide group).^[1] Thanks to their rigid inorganic cores, POSS are endowed with considerable chemical and thermal stability, which can be channeled to their pendant organic groups.

POSS nanoparticles have found novel applications in photonics and electronic devices,^[2] significantly enhancing the thermal, mechanical, and physical properties of the final materials and opening the challenge to synthesize new luminescent hybrid matrices with optoelectronic properties comparable to those of dendronized or grafted conjugated polymers.^[3] POSS nanoparticles can be dispersed at a molecular level (0.5–5 nm)^[4] and, because of their synthetically well-controlled functionalization, can be incorporated into polymers by different polymerization techniques with minimal processing disruption.^[5] This excellent dispersion at the molecular scale and the copolymerization with organic monomers prevents phase separation, thereby ensuring macroscopic homogeneity of the resultant materials.^[6] In this way, new optical hybrid materials based on POSS nanoparticles as the inorganic part overcome some of the most important limitations intrinsic to sol–gel hybrid composites while maintaining the combined physical, chemical, and mechanical advantages of organic–inorganic systems.^[7]

We demonstrated, for the first time, the behavior of POSS-doped systems as disordered nanomaterials, which was to the best of our knowledge a possibility never consid-

[a] M. E. Pérez-Ojeda, Prof. Dr. Á. Costela, Prof. Dr. I. García-Moreno
Instituto Química-Física “Rocasolano”, C.S.I.C.
Serrano 119, 28006 Madrid (Spain)
Fax: (+34) 915642431
E-mail: i.garcia-moreno@iqfr.csic.es

[b] B. Trastoy, Dr. J. L. Chiara
Instituto de Química Orgánica General, C.S.I.C.
Juan de la Cierva 3, 28006 Madrid (Spain)
Fax: (+34) 915644853
E-mail: jl.chiara@iqog.csic.es

[c] Prof. Dr. Í. López-Arbeloa, Dr. J. Bañuelos
Departamento de Química Física
Universidad del País Vasco-EHU
Facultad de Ciencias y Tecnología
Apartado 644, 48080 Bilbao (Spain)
Fax: (+34) 946013500
E-mail: inigo.lopezarbeloa@ehu.es

Supporting information for this article is available on the WWW under <http://dx.doi.org/10.1002/chem.201100512>.

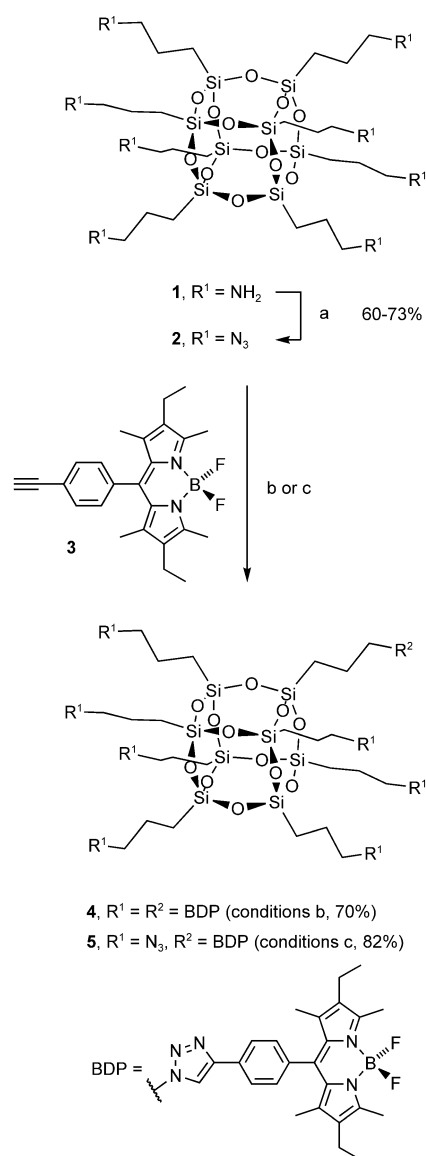
ered before.^[8] The dispersion of POSS nanoparticles at a molecular level defines highly homogeneous materials that, when doped with lasing dyes, allow coherent laser emission but, in addition and in spite of their nanometer size, the POSS particles sustain a weak optical scattering that helps lasing by elongating the light path inside the gain media, thus providing an extra feedback, a phenomenon central to the process called “incoherent random lasing” or “lasing with intensity feedback”.^[9] In this way, the laser action in systems based on dye-doped POSS materials is significantly enhanced, in both the liquid and solid phases.^[7]

The unique chemical and optical properties exhibited by POSS nanoparticles have led us to design new hybrid photonic systems based on POSS labeled with fluorescent dyes as pendant groups on their rigid inorganic cores. Herein, we report the synthesis and characterization of new hybrid organic–inorganic dyes based on azide-functionalized POSS as the inorganic part, and a 4,4-difluoro-4-bora-3a,4a-diaza-*s*-indacene (BDP) chromophore as the organic component, which was selected for its interesting photophysical and photochemical properties both in the liquid phase and in doped solid matrices.^[10] It was anticipated that the new hybrid systems would exhibit highly efficient, stable, and tunable laser emission with improved thermal properties owing to the chemical attachment of the fluorophore to the rigid inorganic framework, strengthening their biomedical and photonic applications. To study the effects of both the linkage group through which BDP is attached to the POSS unit and the degree of functionalization of the inorganic core on the optical properties, we proceeded to synthesize model dyes as well as mono- and octa-substituted BDP–POSS hybrid derivatives.

Results and Discussion

Synthesis and characterization

We recently described the synthesis of octakis(3-azidopropyl)octasilsesquioxane (**2**), a highly symmetrical and topologically ideal cube-octameric POSS monomer containing eight azide groups (Scheme 1).^[11] Compound **2** could be readily obtained in one-step from commercially available octakis(3-aminopropyl)octasilsesquioxane (**1**) using a highly efficient diazo-transfer reaction promoted by nonafllyl azide,^[12] a shelf-stable diazo-transfer reagent. The very mild conditions of this reaction prevented nucleophile-induced cage rearrangements,^[13] which are common in alternative routes to **2** involving nucleophilic substitution reactions with azide ion.^[14] Compound **2** is an excellent nano building block for the synthesis of new functional nanocages with perfect 3D cubic symmetry through copper(I)-catalyzed 1,3-dipolar azide–alkyne cycloaddition (CuAAC)^[15] with a variety of terminal alkynes.^[11,14a,c,d] The versatility of this approach has been demonstrated by the preparation of the dye–POSS cluster **4** using the alkyne-substituted BDP fluorescent dye **3** (Scheme 1).^[11]



Scheme 1. a) CF₃(CF₂)₃SO₂N₃, NaHCO₃, cat. CuSO₄, Et₂O/H₂O/MeOH, RT, 16 h; b) cat. CuSO₄·H₂O, sodium ascorbate, CH₂Cl₂/H₂O, RT, 4.5 h (**2/3** molar ratio = 1:10); c) cat. [Cu(C18₆tren)]Br, *i*Pr₃NEt, toluene, 80 °C (MW), 6 h (**2/3** molar ratio = 10:1).

We have now studied the monofunctionalization of octa-azide **2** with BDP dye **3**. This reaction affords a POSS derivative **5** labeled with a single fluorescent probe and containing seven additional reactive azide groups suitably predisposed for further functionalization with any molecule of interest having a terminal alkynyl group (Scheme 1). Besides, compound **5** would be an interesting hybrid dye for the preparation of solid-state laser materials with improved thermal and chemical stability. Full details of our study of

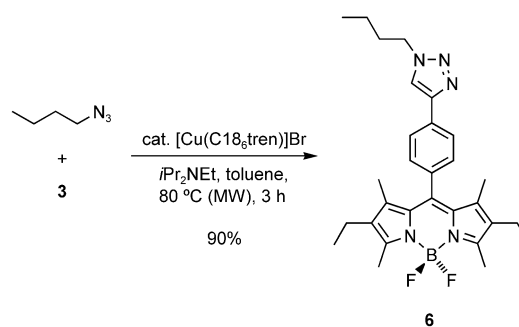
the CuAAC monofunctionalization reaction of octa-azide **2** under different reaction conditions will be published elsewhere. The optimized conditions involved the use of a ten-fold molar excess of **2** over alkyne **3**, to guarantee a high statistical selectivity for the monofunctionalized product **5**, and the recently described^[16] [Cu(C18₆tren)]Br (C18₆tren = tris(2-dioctadecylaminoethyl)amine) catalyst with added Hünig's base in toluene as solvent under microwave heating. These optimized conditions afforded a high yield of **5** (82%), close to the expected statistical value (95.6%). The rest of the alkyne **3** was transformed into a complex mixture of polytriazolyl POSS products, as shown by ¹H NMR analysis of the remaining mixed fractions from column chromatography. The structure of **5** was unambiguously confirmed by its high-resolution mass spectrometry and multinuclear (¹H, ¹³C, ²⁹Si) NMR spectroscopy data (see the Supporting Information).

We have studied the thermal stabilities of POSS derivatives **4** and **5** by thermogravimetric analysis (TGA) (see the Supporting Information). TGA of compound **4** under nitrogen atmosphere showed an initial 7.4% mass loss at about 100 °C attributable to the loss of water from the hygroscopic compound, followed by a 48% mass loss at about 364 °C due to degradation of the POSS itself. In air, the thermogram again showed an initial 5.8% mass loss of water at about 100 °C, followed by a two-stage decomposition process characterized by 26.7% and 48.4% mass losses starting at around 364 °C and 445 °C, respectively, with a final char yield of 14.6% at 800 °C, which is slightly higher than expected for just SiO₂ formation (calculated 11.1%). For comparison, the model BDP dye PM567 (Figure 2) showed an onset decomposition temperature of around 204 °C in its thermogram in air (see the Supporting Information), which is about 160 °C lower than that of hybrid BDP-POSS cluster **4**, confirming our expectations concerning the thermal stabilizing effect of the covalently bonded POSS core. TGA of compound **5** under nitrogen showed a two-stage decomposition process with an onset temperature of about 147 °C and a mass loss of 13.7%, attributed to the loss of seven N₂ molecules from decomposition of the seven azide groups, followed by a second mass loss of 24.7% starting at about 380 °C. In air, an initial 14.0% mass loss was observed starting at about 138 °C, corresponding again to loss of N₂ from the seven azide groups, followed by a 45.7% mass loss starting at about 314 °C, with a final char yield of 34.7% at 800 °C, which is also in this case somewhat higher than expected for SiO₂ formation (calculated 32.2%).

To study the photophysical properties of the BDP-POSS constructs **4** and **5**, we also prepared the new BDP dye **6** as a model system in which a methyl group is attached in place of the POSS core. Compound **6** was readily obtained by the CuAAC reaction of **3** with 1-azidobutane (Scheme 2).

Photophysical and lasing characterization

Studies were carried out to analyze the dependences of both the photophysical properties and the laser performances of



Scheme 2. Synthesis of model BDP dye **6**.

the new BDP dyes on different experimental parameters, such as the linkage group through which the chromophore is attached to the POSS core, the degree of functionalization of the core, the nature of the solvent, and the composition of the host matrix.

Influence of substitution at C-8 of PM567 (compounds **3 and **6**):** Before attaching the BDP derivatives to a POSS core, it is essential to characterize the influence of the linking unit on the photophysics of the BDP chromophore. Hence, appropriate model dyes were firstly analyzed.

Photophysical characterization: The absorption spectra and fluorescence decay curves of model dyes **3** and **6** measured in the same solvent are depicted in Figure 1. In general, the

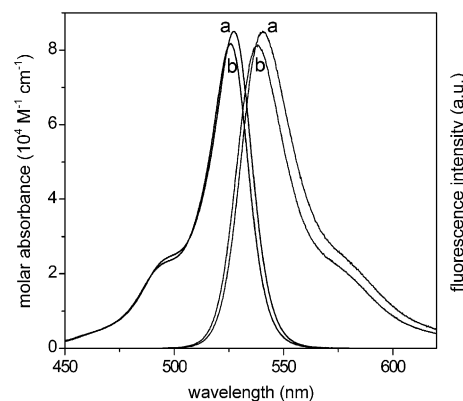
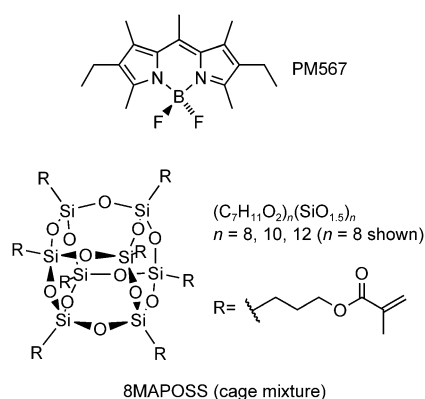


Figure 1. Absorption and fluorescence spectra of compounds **3** (a) and **6** (b) in cyclohexane.

shape and position of the spectral bands of both model dyes bearing *para*-phenyl substituents are similar to those of the parent PM567 dye (Scheme 3)^[17] and other 8-phenyl analogues.^[18] The steric hindrance introduced by the methyl groups flanking the *meso* position of the chromophore hampers the resonant interaction between the electronic clouds of the phenyl group and the BDP core. In fact, such a constrained structure results in an almost perpendicular disposition of the phenyl group with respect to the chromophoric plane, reducing its influence on the BDP core.^[19]



Scheme 3.

Table 1 lists the photophysical properties of dyes **3–6** in a common solvent. For comparison purposes, the corresponding data of the parent BDP dye (PM567), recorded under

Table 1. Photophysical properties of compounds **3**, **4**, **5**, **6**, and PM567 (reference dye)^[17] in cyclohexane.^[a]

Compounds	λ_{abs}	ϵ_{max}	λ_{fl}	ϕ	τ	k_{fl}	k_{nr}
3	527.5	8.5	542.0	0.54	2.96	1.82	1.55
4 ^[b]	523.0	38.0	545.0	0.25	3.66 (59%) 2.15 (24%) 0.35 (17%)	–	–
5	526.0	5.8	540.0	0.60	3.86	1.55	1.03
6	526.0	8.1	540.0	0.67	3.74	1.79	0.88
PM567	522.5	9.3	537.0	0.70	5.60	1.25	0.53

[a] Absorption ($\lambda_{\text{abs}} \pm 0.5$ nm) and fluorescence ($\lambda_{\text{fl}}, \pm 0.5$ nm) wavelength, molar absorption ($\epsilon_{\text{max}}, 10^4 \text{ M}^{-1} \text{ cm}^{-1}$), fluorescence quantum yield ($\phi, \pm 0.05$) and lifetime ($\tau, \pm 0.05$ ns), radiative ($k_{\text{fl}}, 10^8 \text{ s}^{-1}$), and nonradiative ($k_{\text{nr}}, 10^8 \text{ s}^{-1}$) deactivation rate constants. [b] Compound **4** was found to be insoluble in cyclohexane, hence the data shown were obtained in acetone. The full data in different solvents are listed in Tables S1 and S2 in the Supporting Information.

identical experimental conditions, are also included in Table 1 (see also Table S1 in the Supporting Information for photophysical data in different solvents). With respect to the PM567 dye, the presence of a *p*-phenyl group linked to the *meso* position of the BDP core induced a slight bathochromic shift of the absorption and fluorescence bands, an increase in the nonradiative deactivation constant, and, consequently, a slight decrease in the fluorescence quantum yield and lifetime. It has previously been reported that the free rotation of such bulky groups enhances the internal conversion processes, and hence drastically reduces the fluorescence of the dye.^[20] However, in these model dyes, the steric interaction with the flanking methyl groups seems to hinder, at least to some extent, the rotation of the phenyl ring.^[19] In spite of this geometrical restriction, it seems that the phenyl group might have some rotational freedom, increasing the vibrational coupling with the BDP core, which could explain the slight decrease in the fluorescence of the model dyes.^[18]

Laser properties: The lasing behavior of model dyes **3** and **6** was analyzed according to the following protocol. First, we carried out a systematic analysis of the laser action of the new dyes in the liquid phase to guide the selection of the best dye/host matrix combination among the quasi-unlimited compositions and structures of solid materials with a view to optimizing both the lasing efficiency and the photostability.

The dependence of the laser action on the concentration of the new BDP dyes was analyzed in ethyl acetate by varying the dye concentration while keeping the other experimental parameters constant. Under these experimental conditions, broad-line-width laser emission peaked at around 558 nm, with a pump threshold energy of about 0.8 mJ, a beam divergence of about 5 mrad, and a pulse duration of around 8 ns FWHM (full-width at half-maximum), was obtained from the new dyes when placed in a simple plane-plane non-tunable resonator.

Concentrations of $5 \times 10^{-4} \text{ M}$ and $6 \times 10^{-4} \text{ M}$ resulted in the highest lasing efficiencies (defined as the ratio between the energy of the dye laser output and the energy of the pump laser incident on the sample surface) for compounds **3** (61%) and **6** (60%), respectively. The actual effect of the solvent on the dye laser action was analyzed in solutions with concentrations set at the values that optimize the lasing action, using the same solvents that were selected to analyze the photophysical properties of the new dyes. In all of the selected solvents, the model dyes lased with high efficiency (Table 2), their performances exceeding those of the parent dye PM567 (35%) and other 8-substituted BDP dyes when pumped under identical experimental conditions.^[21]

Table 2. Laser properties^[a] of the new 8-functionalized BDP dyes in the liquid phase.

Solvent	Compound 3		Compound 5		Compound 6	
	Eff [%]	λ_{la} [nm]	Eff [%]	λ_{la} [nm]	Eff [%]	λ_{la} [nm]
CF ₃ CH ₂ OH	57	558	47	558	58	558
MeOH	50	563	52	560	50	558
EtOH	52	562	51	562	56	560
EtOAc	61	558	61	560	60	558
acetone	50	559	50	561	52	557
cyclohexane	35	562	25	561	21	555

[a] Eff: energy conversion efficiency, λ_{la} : peak wavelength of the laser emission.

The new dyes proved to be highly photostable since, after 100 000 pump pulses at 10 Hz, compounds **3** and **6** retained 90 and 80% of their initial laser outputs, respectively, which represents a significant improvement in useful lifetime compared with commercial PM567 as well as other 8-substituted BDP dyes when pumped under otherwise identical experimental conditions (Table 2 and Figure 2).^[21] This enhancement may be related to a higher photochemical stabilization of the chromophores rather than to a decline in the nonradiative deactivation processes, since the new dyes have similar values of k_{nr} as the parent PM567. In addition, the lasing behavior of the new dyes showed good correlation with their photophysical properties in dilute solutions. Thus, the

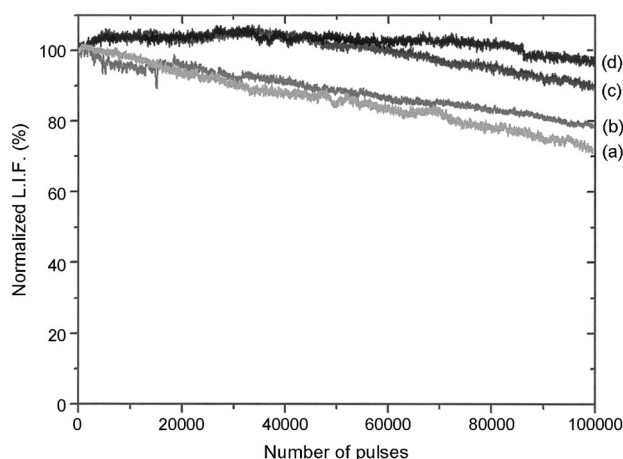


Figure 2. Normalized laser-induced fluorescence emission as a function of the number of pump pulses for PM567 (a), **6** (b), **3** (c), and **5** (d) dye solutions in ethyl acetate. The residual laser-induced fluorescence emissions after 100 000 pulses for (a) to (d) were 71.4, 78.8, 89.5, and 97.3 %, respectively. Pump energy and repetition rate: 5.5 mJ pulse⁻¹ and 10 Hz, respectively.

similarity between the photophysical properties was also manifested in similar laser behavior for both dyes. Looking at the dependence of the laser action of each new dye on the nature of the solvent, it can be appreciated that the higher the fluorescence quantum yield, the higher the lasing efficiency.

The laser action of the new BDP dyes **3** and **6** in the solid state was analyzed in samples synthesized with the dye concentration that induced the highest lasing efficiency in liquid solution (5×10^{-4} to 6×10^{-4} M, depending on the dye). Methyl methacrylate (MMA) was chosen as the main monomeric component of the formulations because this ester mimics ethyl acetate, a solvent in which both model dyes display high lasing efficiencies.

First, compounds **3** and **6** were incorporated as true solutions into the solid homopolymer poly(methyl methacrylate) (PMMA), to delineate the effect of the 8-substituent on their lasing action when pumped under the experimental conditions described above. The results obtained are summarized in Table 3. No significant differences were observed in the wavelength of the maximum laser emission of each dye between their liquid and solid solutions. Lasing efficiencies of 40 and 38 %, respectively, were measured, which are lower than those obtained from the corresponding solutions in ethyl acetate, whereas the lasing photostability main-

tained similar values to those measured in the liquid phase. In this regard, it has to be taken into account that the surface finishes of the solid samples relevant to the laser operation were not laser-grade, which is more detrimental to laser efficiency than to laser photostability. To put the present results into perspective, the lasing parameters of PM567 in PMMA were also measured under the same conditions. The results obtained (a laser efficiency of 28 %, with the emission dropping to zero after 100 000 pump pulses)^[22] were clearly inferior to those obtained for the new 8-functionalized BDP dyes.

The photophysical and lasing properties of the new model BDP dyes in solution indicated that a very polar protic solvent such as 2,2,2-trifluoroethanol would also be a good liquid medium for laser operation. To mimic this solvent, we selected the monomer 2,2,2-trifluoroethyl methacrylate (TFMA) for the preparation of linear copolymers with different proportions of MMA. The incorporation of the new dyes **3** and **6** into this fluorinated organic matrix did not improve their laser performances as compared with those obtained in pure PMMA homopolymer (Table 3). In fact, the presence of the fluorinated monomer in the matrix slightly decreased both the lasing efficiency and the photostability of the dyes. Although photobleaching of dyes can occur through several different mechanisms and, from a general point of view, can be considered to be quite complex, at low irradiances and under ambient atmosphere the primary photodegradation event of chromophores is believed to be photo-oxidation. As a result, factors that accelerate oxygen diffusion, such as the higher oxygen permeability of fluorinated materials, would be expected to reduce the photostability of the new model BDP dyes.

In summary, the two new analogues of dye PM567, compounds **3** and **6**, have demonstrated similar photophysical properties and higher lasing efficiencies and photostabilities than the parent dye PM567, both in the liquid phase and when incorporated into solid matrices. Therefore, the chosen models are suitable candidates to be linked to the POSS unit, since the unique photophysical properties of a BDP chromophore such as PM567 are preserved after the introduction of the alkynyl or 1,2,3-triazolyl substituents at the *para*-position of the phenyl ring. Furthermore, the attachment of the BDP unit to the POSS core is known to be an efficient means of photostabilizing BDP laser dyes.

Influence of the BDP-POSS click assembly—monosubstitution (compound **5**):

Photophysical characterization: The linkage of the BDP moiety to the POSS core (compound **5**) had only a minor effect on the spectral band positions and on the fluorescence lifetime, which remained close to those of the model BDP bearing the linking unit (compound **6**, Table 1). However, the absorption transition probability was more affected by the presence of POSS (the molar absorption decreased by around 25 %) than the fluorescence transition, since the fluorescence quantum yield decreased by only around 10 %

Table 3. Laser properties of the new photosensitized materials.

Material ^[a]	Compound 3			Compound 5			Compound 6		
	Eff [%]	λ_{la} [nm]	I [%]	Eff [%]	λ_{la} [nm]	I [%]	Eff [%]	λ_{la} [nm]	I [%]
A	40	560	97	52	560	100	38	559	77
B	36	560	82				31	558	72
C				56	558	100			

[a] A: PMMA; B: Co(MMA/TFMA, 70:30); C: Co(MMA/8MAPOSS, 87:13).

(Table 1). This behavior may be attributed to a reduction/enhancement of the radiative/nonradiative deactivation processes, respectively, explaining the maintenance of the fluorescence lifetime (Table 1). The reduction of the k_{r} values is correlated with the decrease in the absorption probability, while the enhancement of the k_{nr} values should be related to the large pendant POSS framework. A molecular structure with high conformational freedom increases the flexibility of the dye, thereby favoring internal conversion processes.^[20] In any case, the resulting hybrid dye retained a high fluorescence capacity (up to 0.65, with lifetimes of around 4–6 ns; see Table S1 in the Supporting Information).

Laser properties: The laser action of the new hybrid dye **5** was evaluated following the protocol described above. Under the selected experimental conditions, a concentration of the new hybrid BDP dye of 7.5×10^{-4} M assured an optical density at the pumping wavelength (532 nm) similar to that selected for the characterization of the 8-functionalized BDP dyes **3** and **6**. The hybrid dye **5** lased at around 560 nm with an efficiency ranging from 60% (ethyl acetate) to 25% (cyclohexane), and showed high photostability with no sign of degradation in its laser output after 100 000 pump pulses at a repetition rate of 10 Hz (Table 2 and Figure 2). It should be noted that although the lasing performances of dyes **5** and **3** were similar, the absorption and fluorescence probabilities were lower for the hybrid dye. This fact can be related to our initial hypothesis: the POSS particles, with sizes below 5 nm, act as weak scattering centers in the Rayleigh limit (particle size much smaller than the emission wavelength), increasing the effective optical path inside the gain medium in a process known as non-resonant feedback (NRF) lasing, incoherently supplementing the conventional laser action in such a way as to increase the efficiency of the laser system.^[8,23] Under laser irradiation, the opening up of this new non-resonant feedback pathway explains the high laser performance of the new BDP–POSS cluster, as well as the lack of correlation with its photophysical properties, which were recorded under much lower excitation intensities.

Incorporation of the new BDP–POSS dye into PMMA remarkably improved the laser action as compared to that recorded with dye **3** in the same matrix (material A, Table 3). Thus, for the hybrid dye, a laser efficiency as high as 52% was recorded, without any sign of degradation after 100 000 pump laser pulses in the same position of the sample at a repetition rate of 10 Hz. The incorporation of methacryl-POSS nanoparticles (8MAPOSS cage mixture, Scheme 3) into this medium resulted in a further enhancement of the lasing performance. In this way, a new solid material based on a copolymer of MMA with a 13% weight ratio of 8MAPOSS doped with hybrid dye **5** reached a lasing efficiency of up to 56%, while maintaining a high photostability (material C, Table 3).

To better assess the laser photostability of the new hybrid BDP–POSS dye **5**, we proceeded to carry out a longer run of pumping under more drastic conditions by irradiating the

same position of the sample at a repetition rate of 30 Hz (Figure 3). The new hybrid dye dissolved in pure PMMA exhibited high photostability, without any sign of degradation

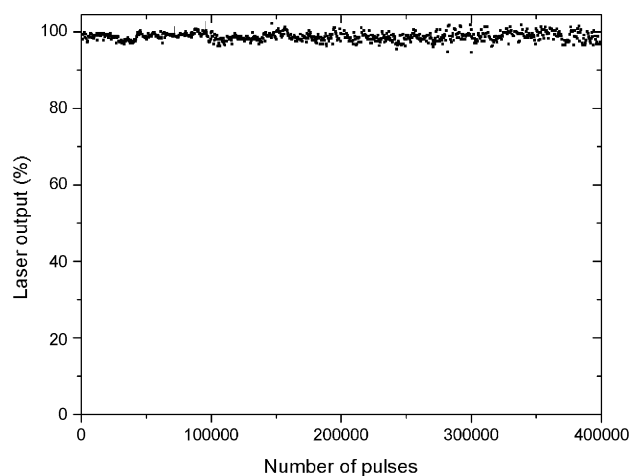


Figure 3. Normalized laser output as a function of the number of pump pulses in the same position of the sample for the new hybrid dye **5** incorporated into PMMA. Pump energy and repetition rate: $5.5 \text{ mJ pulse}^{-1}$ and 30 Hz, respectively.

of its laser output after 400 000 pump pulses. Thus, regarding laser efficiency and photostability, the new hybrid BDP–POSS cluster improved our previous results based on hybrid matrices doped with the parent PM567 dye, even when these matrices were based on copolymers of MMA with different weight ratios of 8MAPOSS.^[22,24]

Influence of the BDP–POSS click assembly—octa-substitution (compound **4**):

Photophysical characterization: This multichromophoric hybrid dye was found to be insoluble in apolar solvents, such that not even dilute (10^{-6} M) solutions could be obtained, but dissolved well in polar media such as acetone, ethyl acetate, and 2,2,2-trifluoroethanol. Figure 4 shows the corresponding absorption and fluorescence spectra, together with the fluorescence decay curves. The presence of eight BDP units in the same molecule led to a large increase in the absorption transition probability, with ϵ_{max} being as high as $38 \times 10^4 \text{ M}^{-1} \text{ cm}^{-1}$ in acetone (Table 1), probably the largest reported for a BDP-based system. The fluorescence properties of compound **4** depended on the nature of the solvent. Indeed, whereas in ethyl acetate the fluorescence quantum yield was high (0.62) and the decay curve could be interpreted as monoexponential with a lifetime of 5.4 ns, an increase in solvent polarity led to a loss of the fluorescence ability, most notably in trifluoroethanol (see Table S2 in the Supporting Information). In acetone, the decay curve became multiexponential, consisting of two components with lifetimes of 2.1 and 3.6 ns (Table 1), which could be assigned to different microenvironments of the BDP units in compound

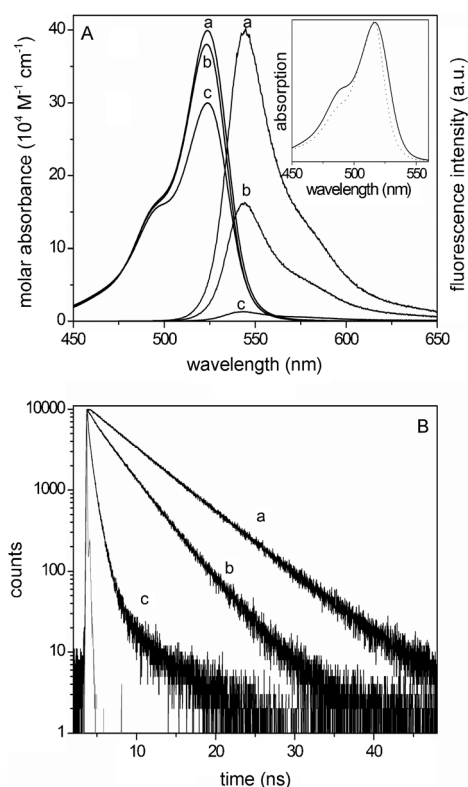


Figure 4. A) Absorption and fluorescence spectra of compound **4** scaled by its molar absorption and fluorescence quantum yields, respectively, in ethyl acetate (a), acetone (b), and trifluoroethanol (c). The normalized absorption spectra of PM567 (dashed) and compound **4** (solid) are also included. B) Fluorescence decay curves.

4 (for instance, a chromophore surrounded by other BDP moieties or by solvent), and a third fast component (0.3 ns) due to a quenching process responsible for the decrease in the fluorescence quantum yield. In the most polar medium, the fluorescence emission was almost negligible and the decay curve was multiexponential and characterized by very short lifetimes.

To gain a deeper insight, we tried to simulate theoretically the most stable ground-state conformation of compound **4** by means of the AM1 semiempirical method. Taking into account the large number of possible conformations of this molecule, we followed two different approaches for the geometry optimization. On the one hand, a full optimization of the octasubstituted POSS was performed starting from a geometry with the BDP chromophores located as far as possible from each other and with the phenyl substituents oriented coplanar to the BDP system. On the other hand, we carried out a sequence of stepwise building of the molecule followed by full geometry optimization at each step starting from the bare octapropyl-POSS core, then adding the eight triazolyl rings and finally four of the eight phenyl-BDP substituents on one of the faces of the POSS cube, to ultimately obtain a simplified model of **4** in an energy-minimized conformation. One should keep in mind the difficulty in handling such large and flexible structures, with many allowed

conformations. In all cases, the final optimized geometry (Figure 5) revealed that the phenyl rings and their attached indacene subunits were not coplanar, as expected. Besides,

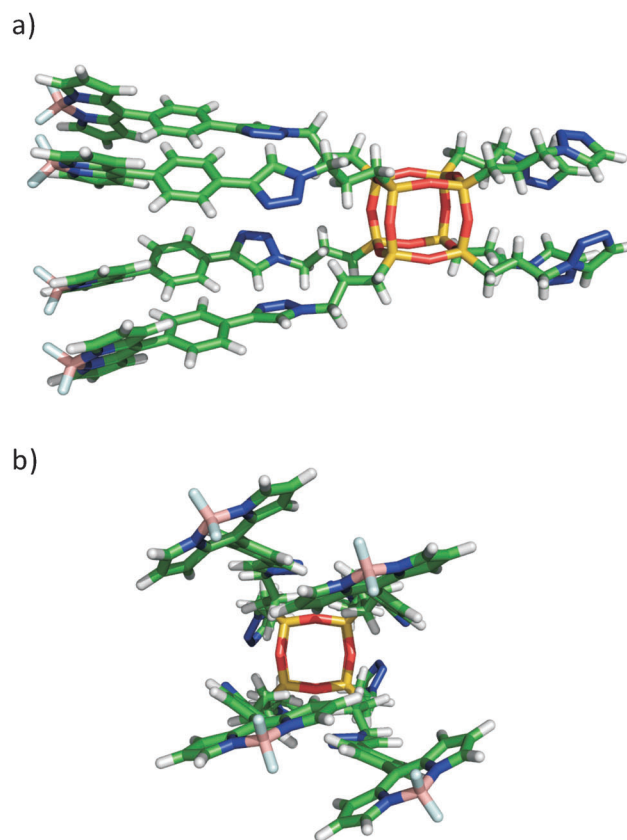


Figure 5. Optimized geometry (at AM1 semiempirical level) of a simplified model of compound **4** lacking four of the eight phenyl-BDP substituents: (a) front view; (b) side view.

the BDP chromophores did not occupy the available free volume, but rather tended to be in close contact, allowing through-space interactions between them. In fact, it was observed that the BDP units tended to be paired, with a cofacial arrangement (Figure 5), allowing a π - π interaction and, consequently, the formation of H-type or “sandwich” aggregates, in which the transition moments of the chromophores are in a parallel arrangement.^[25]

The self-association of the BDP chromophores was corroborated by other experimental findings. Comparison of the normalized absorption spectra of the octasubstituted POSS **4** and the parent PM567 dye indicated that the spectrum of the hybrid material was wider, with increased absorbance in the hypsochromic shoulder region, which is characteristic of H-type aggregates (Figure 4). Besides, the absorption probability of compound **4** does not correspond to the sum of eight BDP units (the ϵ_{\max} of model dye **6** was measured as $8.1 \times 10^4 \text{ M}^{-1} \text{ cm}^{-1}$; Table 1). We have pointed out previously that the linkage of the BDP unit to the POSS core (compound **5**) led to a slight reduction in the absorption transition probability.

Although BDP dyes usually have a low tendency to self-associate,^[20c] some authors have claimed the presence of aggregates in confined environments or in multichromophoric dyes, in which the BDP cores are closely disposed through molecular bridges.^[26] Owing to the hydrophobicity of the BDP dye, an increase in the polarity in the surrounding environment forces the chromophores into closer association, favoring dye aggregation. Indeed, the hypsochromic absorption shoulder was clearer and the calculated molar fraction of the aggregate was higher in polar solvents (trifluoroethanol). Quantum mechanical calculations suggest that in such an H-type dimer, the BDP monomeric units are mutually disposed with a dihedral angle of 8° between them and separated by 5 Å. However, due to the flexibility of the linking chains, the chromophores are not held tightly in a cofacial manner, which leads to a low exciton coupling and a low splitting of the absorption bands of the aggregate,^[27] thus accounting for the only slight changes observed in the absorption spectrum of the octasubstituted POSS compared to that of the free BDP dye (Figure 4). Indeed, a rough estimate of the degree of aggregation^[28] predicts a molar fraction of around 0.8 for the monomer and 0.10 for the dimer (0.20 for the monomeric units of the aggregate).

Aggregation is the main factor responsible for the decrease in the fluorescence ability and the short lifetime in polar media. Apart from the static fluorescence quenching induced by the H-type aggregates due to their inactive absorption in fluorescence, the multi-exponential decay in polar media was indicative of complex excited-state dynamics. Typically, non-fluorescent H-aggregates undergo deactivation of the monomer excited states by energy-transfer processes.^[28] The formation of a fluorescent excimer is ruled out since the recorded fluorescence band resembled that of the model BDP dye, no new fluorescence bands were detected, and the deconvolution of the decay curves was the same regardless of the emission wavelength. Besides, the spatial proximity between the BDP units, as revealed in the optimized geometry of the octasubstituted POSS (Figure 5), could lead to extra quenching processes (i.e., interconversion between aggregates and monomers) producing an overall loss of fluorescence capacity due to the flexibility of the spacer connecting the BDP units to the POSS core, which could allow a range of different relative arrangements of the BDP units contributing to the loss of fluorescence.^[21c] In this sense, the full optimization of compound **4** predicted a slight loss of planarity in the BDP chromophores, showing a butterfly-like distortion along the transversal axis, while in the monosubstituted POSS (compound **5**) the indacene core remained fully planar. This lack of planarity, probably due to the high steric hindrance of such a constrained structure in the octasubstituted POSS, should lead to an increase in the internal conversion probability.^[29] In view of these results, the octasubstituted POSS **4** is deemed to be unsuitable for use as a dye laser.

Laser properties: Hybrid dye **4** did not lase even under drastic pumping conditions. Indeed, all of the abovementioned

nonradiative pathways, mainly due to the presence of aggregates, greatly enhanced the losses in the resonator cavity, preventing the detection of the laser signal.

Conclusion

Octakis(3-azidopropyl)octasilsesquioxane (**2**) is a topologically ideal nano building block for the efficient synthesis of mono- and octa-functionalized fluorescent nanocages through CuAAC reaction with alkyne-substituted BDP dyes. The controlled monofunctionalization of octa-azide **2** with BDP dye **3** resulted in a fluorescently labeled POSS derivative **5** containing seven additional reactive azide groups suitably predisposed for further functionalization through CuAAC with any molecule of interest having a terminal alkynyl group. Full dye-substitution of POSS afforded a hybrid system characterized by low fluorescence ability, mainly in polar media. Quantum mechanical simulation has provided a molecular basis that allows insight into the composition–structure–properties relationship of these hybrid systems. The optimized molecular geometry suggests that the BDP chromophores tend to be paired, leading to aggregation, which effectively quenches both fluorescence and laser emissions. However, the linkage of one BDP unit to the POSS core had only a minor effect on the photophysics of the dye, while significantly improving the laser properties of the final system with respect to those exhibited by the model dyes. In fact, the new hybrid dye exhibited lasing efficiencies of up to 60% (in the liquid phase) and 56% (in solid matrices), with high photostability, since the laser output remained at its initial value under very demanding pumping conditions (4×10^5 pump pulses in the same position of the sample at 30 Hz repetition rate). The new BDP–POSS cluster gives rise to a non-resonant feedback mechanism, which enhances its coherent laser performance. The versatility in the synthesis of the hybrid systems based on dye-linked POSS nanoparticles, together with their improved optical properties and their nanofabrication capability, opens up the possibility of using these new photonic materials as alternative sources for optoelectronic devices, competing with dendronized or grafted polymers.

Experimental Section

General methods for synthesis and chemical characterization: All melting points were measured with a Reicher Jung Thermovar micro-melting apparatus. Proton and carbon-13 nuclear magnetic resonance (¹H NMR and ¹³C NMR) spectra were recorded on a Bruker AMX-300 (300 and 75 MHz, respectively), a Varian INOVA 300 (300 and 75 MHz, respectively), or a Varian INOVA 400 (400 and 100 MHz, respectively) spectrometer. Silicon-29 nuclear magnetic resonance spectra were measured on a Varian INOVA 400 spectrometer (79.5 MHz). Chemical shifts are expressed in parts per million (δ scale) downfield from tetramethylsilane and are referenced to residual peaks of the deuterated NMR solvent used or to internal tetramethylsilane. Data are presented as follows: chemical shift, multiplicity (s=singlet, d=doublet, t=triplet, m= multiplet and/or multiple resonances, br=broad), integration, coupling con-

stants in hertz (Hz), and assignment. Proton and carbon-13 assignments are based on DQ-COSY, HSQC, and HMBC correlation experiments. Thin-layer chromatography (TLC) was performed with Merck silica gel 60 F₂₅₄ plates and Merck aluminum oxide neutral 60 F₂₅₄ plates. Chromatograms were visualized using UV light of wavelengths 254/365 nm. For the detection of azides, the chromatograms were first dipped in a 1% (w/v) solution of Ph₃P in EtOAc, dried at RT, then dipped in a 1% or 5% (w/w) solution of ninhydrin in 95% aqueous EtOH, and finally charred on a hot plate.^[30] Column chromatography was performed with Merck neutral aluminum oxide or Merck silica gel, grade 60, 230–400 mesh. Mass spectra were recorded on a MALDI Voyager-DE PRO time-of-flight (TOF) spectrometer (Applied Biosystems), using a 2,5-dihydroxybenzoic acid matrix, or on an Agilent/HP 1100 LC/MSD spectrometer using ESI or APCI sources. Anhydrous solvents were prepared according to standard methods by distillation over drying agents or by elution through a Pure Solv column-drying system^[31] from Innovative Technology. All other solvents were of HPLC grade and were used as received. All reactions were carried out under magnetic stirring and, if air- or moisture-sensitive, in oven-dried glassware under argon. Microwave irradiation experiments were performed with a single-mode Discover System from CEM Corporation, using standard Pyrex tubes (10 or 35 mL capacity) sealed with a rubber cap.

Materials: Pyrromethene 567 (laser grade, Exciton) with a purity >99% (checked by spectroscopic and chromatographic methods) was used as received. Solvents for laser studies were of spectroscopic grade (Merck, Aldrich, or Sigma) and were used without purification. Linear and cross-linked copolymers were obtained by copolymerization of methyl methacrylate (MMA) with different volumetric proportions of the monofunctional fluorinated monomer 2,2,2-trifluoroethyl methacrylate (TFMA) and of methacryl-POSS (8MAPOSS cage mixture, from Hybrid Plastics). All monomers were purchased from Aldrich. MMA was purified before use, while TFMA and 8MAPOSS were used as received. 2,2'-Azobis(isobutyronitrile) (AIBN) (Acros) was used as a thermal initiator of polymerization. Azido-POSS **2** was prepared as described previously.^[11] Copper(I) catalyst [Cu(C18₈tren)]Br (C18₈tren = tris(2-dioctadecylaminoethyl)amine) was prepared according to described procedures.^[16a]

Compound 4: A solution of CuSO₄·5H₂O (2.5 mg, 0.010 mmol) and sodium ascorbate (9 mg, 0.045 mmol) in water (0.6 mL) was added to a solution of azido-POSS **2** (20 mg, 0.018 mmol) and 4,4-difluoro-8-(4'-ethynylphenyl)-1,3,5,7-tetramethyl-2,6-diethyl-4-bora-3a,4a-diaza-s-indacene (**3**)^[32] (72 mg, 0.178 mmol) in CH₂Cl₂ (0.9 mL). After stirring for 4.5 h at RT, a saturated aqueous solution of EDTA (1 mL) was added, the mixture was vigorously stirred for 30 min, the phases were separated, and the aqueous layer was extracted with CH₂Cl₂ (3 × 3 mL). The organic layers were combined, dried over Na₂SO₄, and the solvent was removed under reduced pressure. The crude residue was purified by flash column chromatography (hexane/EtOAc, 1:5) to afford **4** (54 mg, 70%) as a red powder. M.p. (from CH₂Cl₂): 290 °C (decomposition). *R*_f = 0.75 (hexane/EtOAc, 1:5); ¹H NMR (400 MHz, CDCl₃): δ = 0.68–0.75 (m, 16H; Si-CH₂CH₂CH₂), 0.93 (t, 48H, *J* = 7.4 Hz; 16 × CH₃CH₂), 1.30 (s, 48H; 16 × CH₃-C), 2.13–2.18 (m, 16H; SiCH₂CH₂CH₂), 2.25 (q, 32H, *J* = 7.4 Hz; 16 × CH₂CH₃), 2.51 (s, 48H; 16 × CH₃-C), 4.46 (t, 16H, *J* = 6.9 Hz; SiCH₂CH₂CH₂), 7.32 (d, 16H, *J*_{AB} = 8.2 Hz; 2 × CH Ar), 8.01 (d, 16H, *J*_{AB} = 8.2 Hz; 2 × CH Ar), 8.15 ppm (s, 8H; 1,2,3-triazole); ¹³C NMR (100 MHz, CDCl₃): δ = 8.7 (SiCH₂CH₂CH₂), 11.9 (CH₃), 12.5 (CH₃), 14.6 (CH₃-CH₂), 17.0 (CH₃-CH₂), 24.1 (SiCH₂CH₂CH₂), 52.4 (SiCH₂CH₂CH₂), 120.7 (CH in 1,2,3-triazole), 126.1 (CH phenyl), 129.0 (CH phenyl), 130.1, 131.2, 133.1, 135.8, 137.9, 139.2 (C in 1,2,3-triazole), 147.1, 154.0 ppm; ²⁹Si NMR (79.5 MHz, CDCl₃): δ = -67.1 ppm; UV/Vis (EtOAc): λ_{max} = 523 nm, ε = 432362 mol⁻¹m³cm⁻¹; MALDI-TOF (2,5-dihydroxybenzoic acid matrix): *m/z*: 4304 [M-F]⁺.

Mono-BDP-POSS 5: [Cu(C18₈tren)]Br (2.2 mg, 0.001 mmol) and *i*Pr₂NEt (6.5 μL, 0.037 mmol) were added to a solution of azido-POSS **2** (134 mg, 0.123 mmol) and 4,4-difluoro-8-(4'-ethynylphenyl)-1,3,5,7-tetramethyl-2,6-diethyl-4-bora-3a,4a-diaza-s-indacene (**3**) (5 mg, 0.012 mmol) in toluene (1 mL) under argon. The mixture was stirred for 6 h at 80 °C under microwave irradiation. The solvent was then removed under reduced pressure and the residue was purified by flash column chromatography

(SiO₂; hexane/EtOAc, 12:1 to 5:3) to recover excess starting material **2** (113 mg, 94% recovery of excess **2** employed) and **5** as a red viscous oil (15.1 mg, 82%). *R*_f = 0.61 (hexane/EtOAc, 5:3); ¹H NMR (400 MHz, CDCl₃): δ = 0.71–0.76 (m, 14H; Si-CH₂CH₂CH₂), 0.83–0.98 (m, 2H; Si*CH₂CH₂CH₂), 0.97 (t, 6H, *J* = 7.55 Hz; CH₂CH₂), 1.34 (s, 6H; CH₃-C1, CH₃-C7), 1.66–1.74 (m, 14H; SiCH₂CH₂CH₂), 2.06–2.13 (m, 2H; Si*CH₂CH₂CH₂), 2.30 (q, 4H, *J* = 7.51 Hz; CH₂CH₃), 2.54 (s, 6H; CH₃-C3, CH₃-C5), 3.26 (td, 14H, *J* = 6.83, 1.42 Hz; CH₂N₃), 4.43 (t, 2H, *J* = 7.11 Hz; CH₂-N=N), 7.36 (d, 2H, *J*_{AB} = 8.43 Hz; 2 × CH phenyl), 7.97 (d, 2H, *J*_{AB} = 8.43 Hz; 2 × CH phenyl), 7.86 ppm (s, 1H; 1,2,3-triazole); ¹³C NMR (100 MHz, CDCl₃): δ = 9.3 (SiCH₂CH₂CH₂), 12.6 (CH₃), 12.7 (CH₃), 14.9 (CH₃CH₂), 17.3 (CH₃CH₂), 22.7 (SiCH₂CH₂CH₂), 24.4 (Si*CH₂CH₂CH₂), 52.8 (CH₂-N=N), 53.5 (CH₂N₃), 120.1 (CH, 1,2,3-triazole), 126.4 (CH, phenyl), 129.2 (CH, phenyl), 130.9, 131.3, 133.0, 135.9, 138.5, 139.8 (C in 1,2,3-triazole), 147.4, 154.1 ppm [Si* = silicon atom with the (1,2,3-triazole-1-yl)propyl substituent]; ²⁹Si NMR: δ = -66.92, -66.97, -67.53 ppm (3:4:1 relative intensities); UV/Vis (EtOAc): λ_{max} = 523 nm (ε = 47427 mol⁻¹m³cm⁻¹); MS (API-ESI): *m/z*: 1493.3 [M+H]⁺, 1475.4 [M-NH₄]⁺.

BDP dye 6: a) Synthesis of 1-butylazide: A solution of 1-bromobutane (1.0 g, 7.5 mmol) and NaN₃ (950 mg, 14.6 mmol) in DMF (15 mL) was stirred for 15 h at 120 °C. The mixture was then poured into water and extracted three times with toluene (final concentration 0.04 M assuming the reaction to be quantitative), and the combined extracts were dried (Na₂SO₄) and used without further purification. b) CuAAC reaction: [Cu(C18₈tren)]Br (11 mg, 0.006 mmol) and *i*Pr₂NEt (32 μL, 0.185 mmol) were added to a solution of 1-butylazide in toluene (2.23 mL, 0.04 M, 0.080 mmol) containing 4,4-difluoro-8-(4'-ethynylphenyl)-1,3,5,7-tetramethyl-2,6-diethyl-4-bora-3a,4a-diaza-s-indacene (**3**) (25 mg, 0.062 mmol) under argon. After stirring for 3 h at 80 °C under microwave irradiation, the solvent was removed under reduced pressure and the residue was purified by flash column chromatography (hexane/EtOAc, 1:5) to afford **6** as a red crystalline powder (28 mg, 90%). *R*_f = 0.44 (hexane/EtOAc, 5:3); m.p. (from EtOAc): 232–235 °C; ¹H NMR (400 MHz, CDCl₃): δ = 0.98 (t, 6H, *J* = 7.5 Hz; CH₂CH₃), 1.00 (t, 3H, *J* = 7.3 Hz; CH₃(CH₂)₃N), 1.34 (s, 6H; CH₃-C1, CH₃-C7), 1.37–1.49 (m, 2H; CH₂(CH₂)₂N), 1.88–2.04 (m, 2H; CH₂CH₂N), 2.31 (q, 4H, *J* = 7.5 Hz; CH₂CH₃), 2.54 (s, 6H; CH₃-C3, CH₃-C5), 4.44 (t, 2H, *J* = 7.2 Hz; CH₂N), 7.35 (d, 2H, *J*_{AB} = 8.3 Hz; CH phenyl), 7.84 (s, 1H; 1,2,3-triazole), 7.97 ppm (d, 2H, *J*_{AB} = 8.3 Hz; CH phenyl); ¹³C NMR (100 MHz, CDCl₃): δ = 12.1 (CH₂CH₃), 12.7 (CH₃-C1, CH₃-C7), 13.7 (CH₃-C3, CH₃-C5), 14.8 (CH₃(CH₂)₃N), 17.2 (CH₂CH₃), 19.9 (CH₂(CH₂)₂N), 32.5 (CH₂CH₂N), 50.4 (CH₂N), 119.9 (CH in 1,2,3-triazole), 126.4 (CH phenyl), 129.0 (CH phenyl), 130.9, 131.4, 133.0, 135.7, 138.5, 139.9, 147.2, 153.9 ppm; UV/Vis (EtOAc): λ_{max} (ε) = 522 nm (108900 mol⁻¹m³cm⁻¹); MS (API-ESI): *m/z*: 504.3 [M]⁺.

Preparation of solid polymeric samples: The new BDP derivatives were incorporated into different solid matrices according to a previously described procedure.^[33] Solid monolith laser samples were cast in cylindrical shape so as to form rods of 10 mm in diameter and 10 mm in length. A cut was made parallel to the axis of the cylinder to obtain a lateral flat surface of ≈ 6 × 10 mm. This surface, as well as the ends of the laser rods, was prepared for lasing experiments by using a grinding and polishing machine (Phoenix Beta 4000, Buehler) until an optical-grade finish was obtained. The planar grinding stage was carried out with Texmet 1000 sandpaper (Buehler) using a diamond polishing compound of 6 μm as an abrasive in mineral oil as a lubricant. The final polishing stage was realized with a G-Tuch Microcloth (Buehler), using a Mastertex cloth disk (Buehler) with diamond of 1 μm in mineral oil as an abrasive.

Photophysical properties: Photophysical properties were measured from dilute solutions of the dyes (around 2 × 10⁻⁶ M), prepared by adding the corresponding solvent to the residue from an appropriate amount of a concentrated stock solution in acetone, after vacuum evaporation of this solvent. UV/Vis absorption and fluorescence spectra were recorded on a Cary 4E spectrophotometer and on a SPEX Fluorolog 3–22 spectrofluorimeter, respectively. Fluorescence quantum yields (φ) were evaluated from corrected spectra, using a diluted solution of PM567 dye (Exciton, laser grade) (φ = 0.91 in methanol) as a reference.^[17] Radiative decay curves were recorded by the time-correlated single-photon counting tech-

nique (Edinburgh Instruments, model FL920). Fluorescence emission was monitored at the maximum emission wavelength after excitation at 470 nm by means of a diode laser (PicoQuant, model LDH470) with 150 ps FWHM pulses. The fluorescence lifetime (τ) was obtained after deconvolution of the instrumental response signal from the recorded decay curves by means of an iterative method. The goodness of the exponential fit was assessed by statistical parameters (chi-squared, Durbin–Watson, and analysis of the residuals). The rate constants of radiative (k_r) and nonradiative (k_{nr}) deactivation were calculated according to $k_r = \phi/\tau$ and $k_{nr} = (1 - \phi)/\tau$, respectively.

The ground-state geometries of the BDP–POSS hybrid dyes in the gas phase were fully optimized by the semiempirical AM1 method implemented in the Gaussian 09 software, compiled in an informatic cluster.

Lasing properties: Liquid solutions of dyes were contained in 1 cm optical-path quartz cells that were carefully sealed to avoid solvent evaporation during experiments. Both the liquid cells and the solid samples were transversely pumped at 532 nm with 5.5 mJ, 6 ns FWHM pulses from a frequency-doubled, Q-switched Nd:YAG laser (Monocrom OPL-10) at a repetition rate of up to 10 Hz. Most representative samples were also pumped at 30 Hz with 3.5 mJ, 10 ns FWHM pulses from a diode-pumped, frequency-doubled, Q-switched Nd:YAG laser (Monocrom HALAZEN 532-12). Details of the experimental system can be found elsewhere.^[24]

The photostability of each dye in the liquid phase was also evaluated under experimental conditions identical to those selected to irradiate the fluorophores embedded in solid polymeric matrices, to allow later comparison of their stabilities in the liquid and solid phases under laser irradiation. Because the irradiated volume in solid samples was estimated to be 10 μ L, capillary tubes charged with solutions of the dyes in ethyl acetate offered the best geometry to reproduce the volume irradiated in the solid samples, maintaining the same laser pump conditions in both cases. Although the low optical quality of the capillary prevented laser emission from the dyes, information about photostabilities could be obtained by monitoring the decrease in laser-induced fluorescence intensity under excitation transverse to the capillary as a function of the number of pump pulses at 10 Hz repetition rate. The fluorescence emission was monitored perpendicular to the exciting beam, and its collection and analysis was carried out with the same set-up selected to characterize the laser emission from dyes incorporated into solid samples.

Acknowledgements

We thank the Spanish Ministerio de Ciencia e Innovación (projects MAT2007-65778-C02-01, MAT2007-65778-C02-02, TRACE2009-0144, CTQ-2006-15515-C02, CTQ2009-14551-C02-02, MAT2010-20646-C04-01, MAT2010-20646-C04-03, and MAT2010-20646-C04-04), the Comunidad de Madrid (project S2009/PPQ-1634 “AVANCAT”), and Gobierno Vasco (IT339-10) for financial support. We also thank the Ministerio de Ciencia e Innovación for an FPU predoctoral fellowship to B.T. and the C.S.I.C. for a JAE-PREDOC fellowship to M.E.P.-O. The SGI/IZO-SGIker UPV/EHU is gratefully thanked for allocation of computational resources.

- [1] For pioneering reports on POSS, see: a) D. W. Scott, *J. Am. Chem. Soc.* **1946**, *68*, 356–358; b) A. J. Barry, W. H. Daudt, J. J. Domicone, J. W. Gilkey, *J. Am. Chem. Soc.* **1955**, *77*, 4248–4252; for reviews, see: c) R. M. Laine, M. F. Roll, *Macromolecules* **2011**, *44*, 1073–1109; d) D. B. Cordes, P. D. Lickiss, F. Rataboul, *Chem. Rev.* **2010**, *110*, 2081–2173; e) P. D. Lickiss, F. Rataboul, *Adv. Organomet. Chem.* **2008**, *57*, 1–116; f) M. G. Voronkov, V. I. Lavrent'yev, *Top. Curr. Chem.* **1982**, *102*, 199–236.
- [2] For a recent review, see: a) K. L. Chan, P. Sonar, A. Sellinger, *J. Mater. Chem.* **2009**, *19*, 9103–9120; for recent work in this field, see: b) M. F. Roll, J. W. Kampf, R. M. Laine, *Macromolecules* **2011**, *44*, 3425–3435; c) X. Yang, J. D. Froehlich, H. S. Chae, B. T. Harding, S. Li, A. Mochizuki, G. E. Jabbour, *Chem. Mater.* **2010**, *22*, 4776–4782; d) N. R. Vautravers, P. Andre, A. M. Z. Slawin, D. J. Cole-Hamilton,

- Org. Biomol. Chem.* **2009**, *7*, 717–724; e) S. Sulaiman, A. Bhaskar, J. Zhang, R. Guda, T. Goodson III, R. M. Laine, *Chem. Mater.* **2008**, *20*, 5563–5573; f) M. F. Roll, M. Z. Asuncion, J. Kampf, R. M. Laine, *ACS Nano* **2008**, *2*, 320–326; g) M. Y. Lo, C. Zhen, M. Lauters, G. E. Jabbour, A. Sellinger, *J. Am. Chem. Soc.* **2007**, *129*, 5808–5809; h) J. D. Froehlich, R. Young, T. Nakamura, Y. Ohmori, S. Li, A. Mochizuki, M. Lauters, G. E. Jabbour, *Chem. Mater.* **2007**, *19*, 4991–4997.
- [3] a) E. Markovic, S. Clarke, J. Matison, G. P. Simon, *Macromolecules* **2008**, *41*, 1685–1692; b) C. Zhao, X. Yang, X. Wu, X. Liu, X. Wang, L. Lu, *Polym. Bull.* **2008**, *60*, 495–505.
- [4] S. Bizet, J. Galy, J. F. Gerard, *Macromolecules* **2006**, *39*, 2574–2583.
- [5] a) L. Zheng, A. J. Waddon, R. J. Farris, E. B. Coughlin, *Macromolecules* **2002**, *35*, 2375–2379; b) E. T. Kopesky, T. S. Haddad, R. E. Cohen, G. H. McKinley, *Macromolecules* **2004**, *37*, 8992–9004; c) K. Y. Pu, B. Zhang, Z. Ma, P. Wang, X. Y. Qi, R. F. Chen, L. H. Wang, Q.-L. Fan, W. Huang, *Polymer* **2006**, *47*, 1970–1978.
- [6] S. Bizet, J. Galy, J. F. Gerard, *Polymer* **2006**, *47*, 8219–8227.
- [7] O. García, R. Sastre, I. García-Moreno, V. Martin, A. Costela, *J. Phys. Chem. C* **2008**, *112*, 14710–14713.
- [8] A. Costela, I. García-Moreno, L. Cerdan, V. Martin, O. Garcia, R. Sastre, *Adv. Mater.* **2009**, *21*, 4163–4166.
- [9] S. Takeda, M. Obara, *Appl. Phys. B* **2009**, *94*, 443–450.
- [10] a) A. Loudet, K. Burgess, *Chem. Rev.* **2007**, *107*, 4891–4932; b) R. Ziessel, G. Ulrich, A. Harriman, *New J. Chem.* **2007**, *31*, 496–501; c) F. L. Arbeloa, J. Banuelos, V. Martinez, T. Arbeloa, I. L. Arbeloa, *Trends Phys. Chem.* **2008**, *13*, 101–122; d) G. Ulrich, R. Ziessel, A. Harriman, *Angew. Chem.* **2008**, *120*, 1202–1219; *Angew. Chem. Int. Ed.* **2008**, *47*, 1184–1201; e) A. C. Benniston, G. Copley, *Phys. Chem. Chem. Phys.* **2009**, *11*, 4124–4131.
- [11] B. Trastoy, M. E. Pérez-Ojeda, R. Sastre, J. L. Chiara, *Chem. Eur. J.* **2010**, *16*, 3833–3841.
- [12] a) J. R. Suárez, B. Trastoy, M. E. Pérez-Ojeda, R. Marín Barrios, J. L. Chiara, *Adv. Synth. Catal.* **2010**, *352*, 2515–2520; for an earlier example of a primary amine to azide transformation using this reagent, see: b) S. Yekta, V. Prisyazhnyuk, H.-U. Reissig, *Synlett* **2007**, 2069–2072; for the synthesis and stability of NiN₃, see ref. [11] and the following: c) N. D. Volkov, V. P. Nazaretyan, L. M. Yagupol'skii, *Zh. Org. Khim.* **1982**, *18*, 519–525; d) S. Zhu, *Tetrahedron Lett.* **1992**, *33*, 6503–6504; e) S.-Z. Zhu, *J. Chem. Soc. Perkin Trans. 1* **1994**, 2077–2081.
- [13] E. Rikowski, H. C. Marsmann, *Polyhedron* **1997**, *16*, 3357–3361.
- [14] For recent alternative routes to **2** by nucleophilic substitution with concomitant partial cage rearrangements, see: a) Z. Ge, D. Wang, Y. Zhou, H. Liu, S. Liu, *Macromolecules* **2009**, *42*, 2903–2910; b) V. Ervithayasuporn, X. Wang, Y. Kawakami, *Chem. Commun.* **2009**, 5130–5132; for improved conditions that largely avoid cage rearrangements, see: c) S. Fabritz, D. Heyl, V. Bagutski, M. Empting, E. Rikowski, H. Frauendorf, I. Balog, W.-D. Fessner, J. J. Schneider, O. Avrutina, H. Kolmar, *Org. Biomol. Chem.* **2010**, *8*, 2212–2218; d) D. Heyl, E. Rikowski, R. C. Hoffmann, J. J. Schneider, W.-D. Fessner, *Chem. Eur. J.* **2010**, *16*, 5544–5548.
- [15] For pioneering reports on CuAAC reactions, see: a) C. W. Tornoe, C. Christensen, M. Meldal, *J. Org. Chem.* **2002**, *67*, 3057–3064; b) V. V. Rostovtsev, L. G. Green, V. V. Fokin, K. B. Sharpless, *Angew. Chem.* **2002**, *114*, 2708–2711; *Angew. Chem. Int. Ed.* **2002**, *41*, 2596–2599; for a comprehensive review, see: M. Meldal, C. W. Tornoe, *Chem. Rev.* **2008**, *108*, 2952–3015.
- [16] a) G. Barré, D. Taton, D. Lastecoueres, J.-M. Vincent, *J. Am. Chem. Soc.* **2004**, *126*, 7764–7765; b) N. Candelon, D. Lastecoueres, A. K. Diallo, J. Ruiz Aranzas, D. Astruc, J.-M. Vincent, *Chem. Commun.* **2008**, 741–743.
- [17] F. López Arbeloa, T. López Arbeloa, I. López Arbeloa, I. García-Moreno, A. Costela, R. Sastre, F. Amat-Guerri, *Chem. Phys.* **1998**, *236*, 331–341.
- [18] J. Bañuelos Prieto, F. López Arbeloa, V. Martínez Martínez, T. Arbeloa López, F. Amat-Guerri, M. Liras, I. López Arbeloa, *Chem. Phys. Lett.* **2004**, *385*, 29–35.

- [19] a) S. Mula, A. K. Ray, M. Banerjee, T. Chaudhuri, K. Dasgupta, S. Chattopadhyay, *J. Org. Chem.* **2008**, *73*, 2146–2154; b) Q. Zheng, G. Xu, P. N. Prasad, *Chem. Eur. J.* **2008**, *14*, 5812–5819; c) T. T. Vu, S. Badré, C. Dumas-Verdes, J.-J. Vachon, C. Julien, P. Audebert, E. Y. Senotrusova, E. Y. Schmidt, B. A. Trofimov, R. B. Pansu, G. Clavier, R. Méallet-Renault, *J. Phys. Chem. C* **2009**, *113*, 11844–11855.
- [20] a) A. Burghart, H. Kim, M. B. Welch, L. H. Thoresen, J. Reibenspies, K. Burgess, *J. Org. Chem.* **1999**, *64*, 7813–7819; b) M. A. H. Alamiry, A. C. Benniston, G. Copley, K. J. Elliot, A. Harriman, B. Stewart, Y.-G. Zhi, *Chem. Mater.* **2008**, *20*, 4024–4032; c) F. López Arbeloa, J. Bañuelos, V. Martínez, T. Arbeloa, I. López Arbeloa, *Int. Rev. Phys. Chem.* **2005**, *24*, 339–374.
- [21] a) F. López Arbeloa, J. Bañuelos Prieto, I. López Arbeloa, A. Costela, I. García-Moreno, C. Gómez, F. Amat-Guerri, M. Liras, R. Sastre, *Photochem. Photobiol.* **2003**, *78*, 30–36; b) I. García-Moreno, A. Costela, L. Campo, R. Sastre, F. Amat-Guerri, M. Liras, F. López Arbeloa, J. Bañuelos Prieto, I. López Arbeloa, *J. Phys. Chem. A* **2004**, *108*, 3315–3323; c) M. Álvarez, A. Costela, I. García-Moreno, F. Amat-Guerri, M. Liras, R. Sastre, F. López Arbeloa, J. Bañuelos Prieto, I. López Arbeloa, *Photochem. Photobiol. Sci.* **2008**, *7*, 802–813.
- [22] R. Sastre, V. Martín, L. Garrido, J. L. Chiara, B. Trastoy, O. García, A. Costela, I. García-Moreno, *Adv. Funct. Mater.* **2009**, *19*, 3307–3316.
- [23] L. Cerdán, A. Costela, I. García-Moreno, O. García, R. Sastre, *Opt. Express* **2010**, *18*, 10247–10256.
- [24] A. Costela, I. García-Moreno, D. del Agua, O. García, R. Sastre, *J. Appl. Phys.* **2007**, *101*, 073110–073120.
- [25] a) E. G. McRae, M. Kasha, *Physical Processes in Radiation Biology*, Academic Press, New York, **1964**; b) J. E. Selwyn, J. I. Steinfeld, *J. Phys. Chem.* **1972**, *76*, 762–774.
- [26] a) F. Bergström, I. Mikhalyov, P. Hagglöf, R. Wortmann, T. Ny, L. B.-A. Johansson, *J. Am. Chem. Soc.* **2002**, *124*, 196–204; b) D. Tleugabulova, Z. Zhang, J. D. Brennan, *J. Phys. Chem. B* **2002**, *106*, 13133–13138; c) M. Bröring, R. Krüger, S. Link, C. Kleeberg, S. Köhler, X. Xie, B. Ventura, L. Flamigni, *Chem. Eur. J.* **2008**, *14*, 2976–2983.
- [27] A. C. Benniston, G. Copley, A. Harriman, D. Howgegeo, R. W. Harrington, W. Clegg, *J. Org. Chem.* **2010**, *75*, 2018–2027.
- [28] I. López Arbeloa, *J. Chem. Soc.* **1981**, *77*, 1725–1733.
- [29] K. H. Drexhage, in *Dye Lasers* (Ed.: F. P. Schäfer), Springer, Berlin, **1990**, Chapter 5, pp. 155–200.
- [30] S. Punna, M. G. Finn, *Synlett* **2004**, 99–100.
- [31] A. B. Pangborn, M. A. Giardello, R. H. Grubbs, R. K. Rosen, F. J. Timmers, *Organometallics* **1996**, *15*, 1518–1520.
- [32] a) G. Ulrich, R. Ziessel, *J. Org. Chem.* **2004**, *69*, 2070–2083; b) V. A. Azov, A. Schlegel, F. Diederich, *Angew. Chem.* **2005**, *117*, 4711–4715; *Angew. Chem. Int. Ed.* **2005**, *44*, 4635–4638.
- [33] M. Álvarez, F. Amat-Guerri, A. Costela, I. García-Moreno, C. Gómez, M. Liras, R. Sastre, *Appl. Phys. B* **2005**, *80*, 993–1006.

Received: February 15, 2011

Revised: July 21, 2011

Published online: October 20, 2011